Progress In Electromagnetics Research M, Vol. 77, 205–213, 2019

Analysis and Compensation of Ionospheric Time-Variant TEC Effect on GEO SAR Focusing

Xingyu Liang and Zhuo Li*

Abstract—Compared to low Earth orbit (LEO) synthetic aperture radar (SAR), geosynchronous (GEO) SAR has a larger coverage and shorter revisit period. However, due to its longer integration time it will be affected by ionospheric time-variant total electron content (TEC), which introduces a phase error into the SAR azimuth signal. Using U.S. total electron content (USTEC) data, TEC variation with time on GEO SAR track is analyzed. It is shown that quadratic phase error caused by time-variant TEC is main effect on image focusing compared to higher order errors. Therefore, contrast optimization autofocus (COA) algorithm can be used for compensation. The key steps of COA are given. Simulations based on scenes derived from PALSAR2 data demonstrate the effectiveness of COA.

1. INTRODUCTION

The concept of geosynchronous (GEO) synthetic aperture radar (SAR) is proposed by Tomiyasu in 1978 [1]. It operates in a geosynchronous orbit (altitude 36000 km) and has a large coverage with a very short repeat period 24 h [2, 3]. Due to its advantages GEO SAR can be well applied in topographic mapping water resource monitoring and soil moisture determination, etc. [1, 4]. For example, a GEO SAR system called Geosynchronous Earth Monitoring by Interferometry and Imaging (GEMINI) was put forward in 2012 to acquire Earth surface data [5, 6]. For GEO SAR, ionospheric effect is an unavoidable problem because its operating frequency is L-band, and it is more sensitive to ionospheric effect compared to higher bands. Unlike low Earth orbit (LEO) SAR, time-variant total electron content (TEC) will have a special effect on GEO SAR because the integration time of GEO SAR is much longer than LEO SAR. The TEC may introduce a second or higher order phase errors in the SAR azimuth signal which will make the SAR image defocusing [7–10].

Here, we use U.S. total electron content (USTEC) data to analyze the time-variant TEC effect. According to the analysis results, contrast optimization autofocus (COA) algorithm is used for compensating the error. After the introduction of principle of time-variant TEC effect in Section 2, the analysis results based on USTEC data are given in Section 3. COA algorithm is presented in Section 4. The effectiveness of COA is tested using simulations based on PALSAR2 data in Section 5.

2. TIME-VARIANT TEC EFFECT ON GEO SAR

According to the theory of electromagnetic wave propagation in ionosphere, ionosphere will introduce a two-way phase ϕ to the transionospheric SAR signal [11, 12]

$$\phi = \frac{4\pi K \cdot TEC}{cf} \tag{1}$$

Received 23 November 2018, Accepted 3 January 2019, Scheduled 14 January 2019
* Corresponding author: Zhuo Li (lizhuo@cugb.edu.cn).
The authors are with the School of Information Engineering, China University of Geosciences, Beijing, China.

where $K = 40.28$, c is the light speed, f the signal frequency, and TEC the total electron content along signal propagation path. This phase is added in phase spectrum of the SAR range signal. It can be expanded to Taylor expansion up to second order terms at carrier frequency $f = f_c$ as [9]

$$\phi = \frac{4\pi K \cdot TEC}{cf_c} - \frac{4\pi K \cdot TEC}{cf_c^2}(f - f_c) + \frac{4\pi K \cdot TEC}{cf_c^3}(f - f_c)^2 \quad |f - f_c| \le \frac{B}{2} \tag{2}$$

where B is the signal bandwidth, and the terms of third and higher orders are ignored. Here we consider the TEC in Eq. (2) is background ionosphere TEC. The second term is a linear phase which will cause a time delay in range. The third term is a quadratic phase which will cause defocusing in range. These two effects are not discussed in this paper.

We focus on the first term in Eq. (2). It is constant in range signal, but the TEC may vary with time in the integration time of GEO SAR, and this phase becomes an error in azimuth signal as

$$\phi(t) = \frac{4\pi K \cdot TEC(t)}{cf_c} \tag{3}$$

where we can use polynomial to approximately express the time-variant TEC as [7]

$$TEC(t) = TEC_0 + k_1 t + k_2 t^2 + k_3 t^3 + \dots \tag{4}$$

in which TEC_0 is constant; k_i is the coefficient of the ith order; and t is the azimuth time. The first order term causes azimuth shift. The second and third order terms cause azimuth defocusing. The higher order may have negligible effect.

According to the acceptable level of quadratic phase error (QPE) and cubic phase error (CPE) to ensure image focusing, i.e., QPE and CPE should be less than $\pi/4$ and $\pi/8$ respectively [7, 13], the requirements for k_2 and k_3 are

$$k_2 \le \frac{cf_c}{4KT_s^2} \tag{5}$$

$$k_3 \le \frac{cf_c}{4KT_s^3} \tag{6}$$

in which T_s is the SAR integration time.

3. ANALYSIS OF TIME-VARIANT TEC EFFECT BASED ON USTEC DATA

Here, we use USTEC data published by the National Oceanic and Atmospheric Administration (NOAA) to analyze time-variant TEC error since it has a high time resolution 15 min.

Firstly, assume that GEO SAR has typical parameters shown in Table 1, and imaging region is U.S. Then, we have the SAR track shown in Fig. 1. The red line is the nadir track, and the blue dashed line is the beam pointing track.

Five positions (points A, B, C, D, E, see Fig. 1) on the SAR track in northern hemisphere are chosen for analysis, for USTEC data is in northern hemisphere. A and E are located in low latitudes on

Table 1. GEO SAR orbit parameters.

Parameters	Values
Orbit semi-major axis (km)	42164.43
Inclination (°)	60
Eccentricity	0
Look angle (°)	3
Wavelength (m)	0.24
Azimuth resolution (m)	5

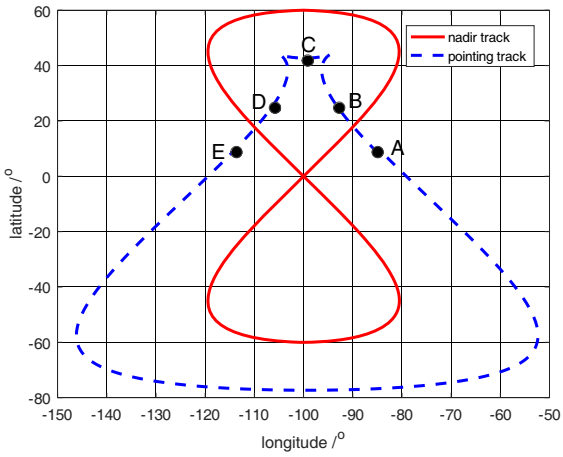

Figure 1. GEO SAR track.

the track, B and D located in middle latitudes, and C is the peak of the track. Through simulation and calculation for 5 m resolution, the SAR integration time at these 5 positions is obtained. Then from Eqs. (5) and (6) the allowed maximum values of k_2 and k_3 are obtained as shown in Table 2. It can be seen that at the peak of pointing track the integration time is longest, and the allowed quadratic and cubic coefficients are smallest.

Table 2. Allowed maximum quadratic and cubic coefficients at 5 positions.

Point	Position	Integration time(s)	Allowed maximum k_2 (TECU/s^2)	Allowed maximum k_3 (TECU/s^3)
A	Lat.10°, Lon.−86°	300	2.6×10^{-6}	8.6×10^{-9}
B	Lat.26°, Lon.−94°	345	2.0×10^{-6}	5.7×10^{-9}
C	Lat.43°, Lon.−100°	520	8.6×10^{-7}	1.7×10^{-9}
D	Lat.26°, Lon.−106°	345	2.0×10^{-6}	5.7×10^{-9}
E	Lat.10°, Lon.−114°	300	2.6×10^{-6}	8.6×10^{-9}

Next, USTEC data in whole year of 2016 are used for fitting TEC variation. The area is from Lat.10° to 60° and Lon.−150° to −50°. The TEC time resolution is 15 min. Eight TEC values in two hours are used for one polynomial fitting. For each position at integer Lat. and Lon. polynomial fitting results are obtained every two hours among all days in 2016. Then we find the maximum quadratic and cubic coefficients (absolute values) of time-variant TEC, which are shown in Figs. 2 and 3. Compared to Table 2, it can be seen that in low latitudes the quadratic coefficients in most areas are larger than the allowed value 2.6×10^{-6}, and all the quadratic coefficients are larger than 2.0×10^{6}, so the quadratic error should be considered. On the other hand, all the cubic coefficients are less than the allowed smallest value 1.7×10^{-9}, so cubic errors can be ignored.

Quadratic coefficient is further analyzed along GEO SAR track with parameters shown in Table 1. For one position, maximum quadratic coefficient is obtained at same local time (LT) in every day, since the repeat period of GEO SAR is 24 h. We also consider that different positions have different local times. For example, if the ascending node time is LT 6am, at equator the maximum quadratic coefficient is found at LT 6am every day, and at the SAR track peak it is found at LT 12am every day. Then we get the result shown in Fig. 4, in which Figs. 4(a)–(d) give the maximum quadratic coefficient in the case of ascending node time LT 0, 6, 12, 18, respectively. The track in Fig. 4 is located at integer Lat. and Lon. Table 3 shows the result at the 5 positions. We compare it to Table 2. For LT 0, the coefficients at A, C are larger than the allowed maximum coefficient. For LT 6, the coefficients at D, E are larger than the threshold. For LT 12, all the coefficients exceed the threshold. For LT 18, A, B, C exceed the threshold. Therefore, quadratic error is unavoidable and should be compensated.

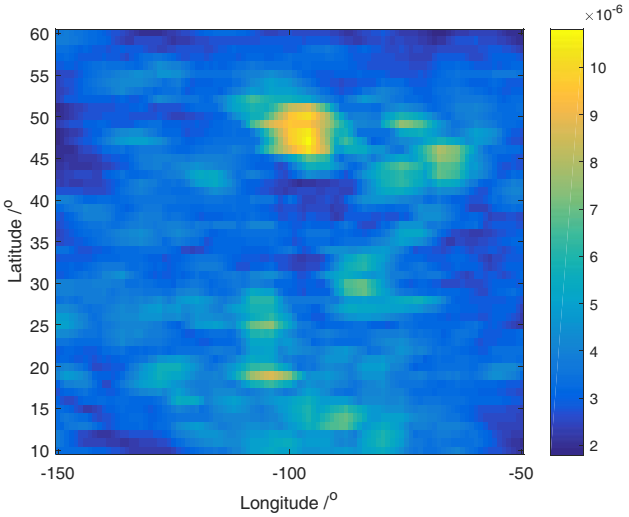

Figure 2. Maximum quadratic coefficient distribution.

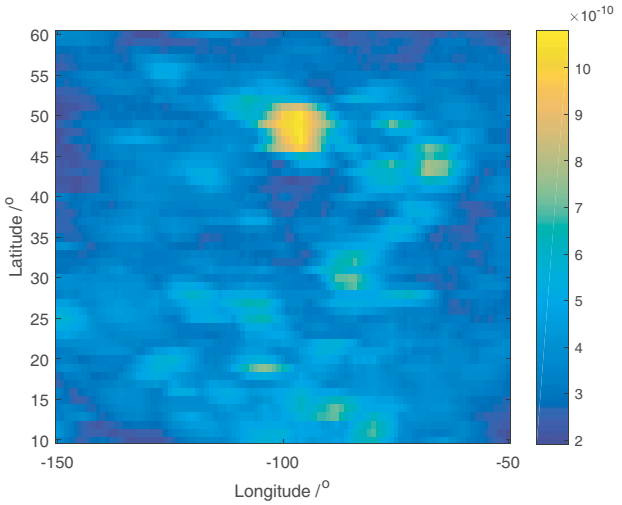

Figure 3. Maximum cubic coefficient distribution.

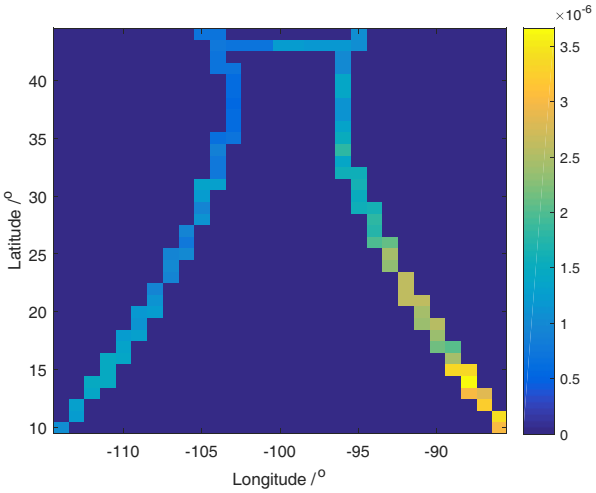

(a) LT 0

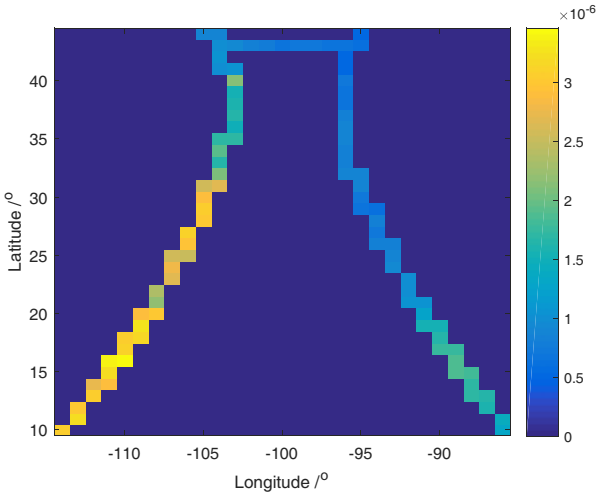

(b) LT 6

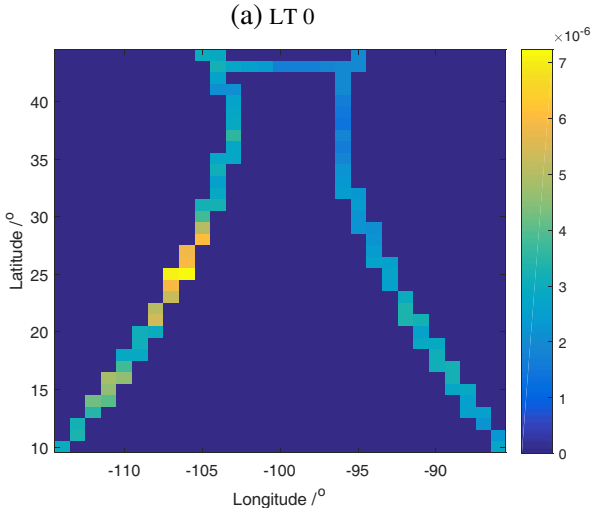

(c) LT 12

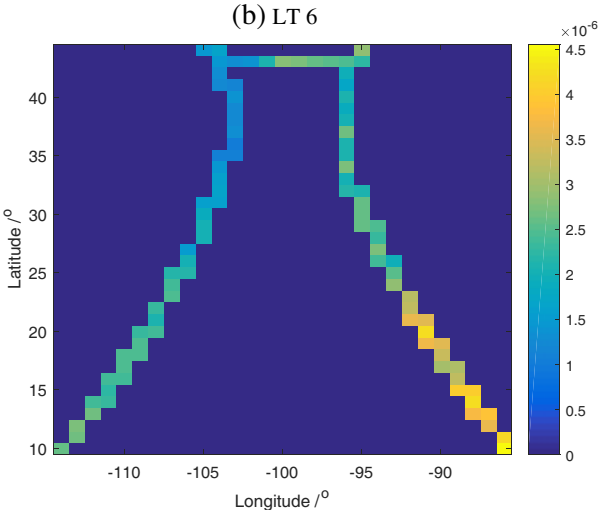

(d) LT 18

Figure 4. Maximum quadratic coefficients along GEO SAR track with different ascending node time.

Table 3. Maximum quadratic coefficients at 5 positions.

Point	Position	Maximum k_2 (TECU/s^2)			
		LT 0	**LT 6**	**LT 12**	**LT 18**
A	Lat.10°, Lon.−86°	3.0×10^{-6}	1.3×10^{-6}	2.8×10^{-6}	4.6×10^{-6}
B	Lat.26°, Lon.−94°	2.0×10^{-6}	8.6×10^{-7}	2.7×10^{-6}	2.4×10^{-6}
C	Lat.43°, Lon.−100°	1.2×10^{-6}	7.0×10^{-7}	1.8×10^{-6}	2.8×10^{-6}
D	Lat.26°, Lon.−106°	7.8×10^{-7}	3.0×10^{-6}	5.9×10^{-6}	2.0×10^{-6}
E	Lat.10°, Lon.−114°	1.1×10^{-6}	3.1×10^{-6}	3.0×10^{-6}	2.6×10^{-6}

4. COA ALGORITHM FOR COMPENSATING TIME-VARIANT TEC ERROR

According to the analysis of time-variant TEC error in U.S., azimuth signal of GEO SAR is mainly affected by quadratic phase error. COA algorithm is originally designed to estimate quadratic phase error in azimuth caused by inaccurate Doppler frequency rate when SAR focusing, so it is applicable to time-variant TEC error compensation. It finds the quadratic coefficient of phase error by means of iteration based on image contrast optimization criterion. Image contrast is defined as

$$C = \frac{\sqrt{E\left\{[I^2 - E(I^2)]^2\right\}}}{E(I^2)} \tag{7}$$

where I is the image amplitude, I^2 the power, and $E(I^2)$ the mean of image power. So the numerator in Eq. (7) is standard deviation of image power, and the denominator is the mean.

The better an image is focused, a larger contrast it will have. Based on this criterion, COA algorithm can find the compensation coefficient when image contrast is optimal. The key steps of COA can be summarized as follows.

1) Range lines selection
   Select range lines with high average power, which probably contain strong targets. Next steps are iterated. An initial quadratic TEC coefficient and its variation step are given.
2) Azimuth signal decompression
   Perform an azimuth fast Fourier transform (FFT) on the range lines selected in 1). Multiply the signal by decompression factor followed by inverse FFT.
3) Quadratic error correction
   Using Eq. (8) to calculate the quadratic phase error $\hat{\phi}(t)$ and correct it in signal.

$$\hat{\phi}(t) = \frac{4\pi K \cdot \hat{k}_2 t^2}{c f_c} \tag{8}$$

   where $\hat{k}_2$ is the current quadratic coefficient.
4) Azimuth signal compression
   Perform azimuth FFT. Multiply the signal by compression factor followed by inverse FFT.
5) Contrast comparison and iteration
   Compare the current contrast to the last one. If it becomes larger, the coefficient step does not change, or else the step takes the opposite number with a half absolute value. Then the coefficient adds one step. 2)–5) process is iterated until the step is less than a given threshold.

   The final quadratic coefficient is used for compensating the error in original image.
   The flowchart is shown in Fig. 5.

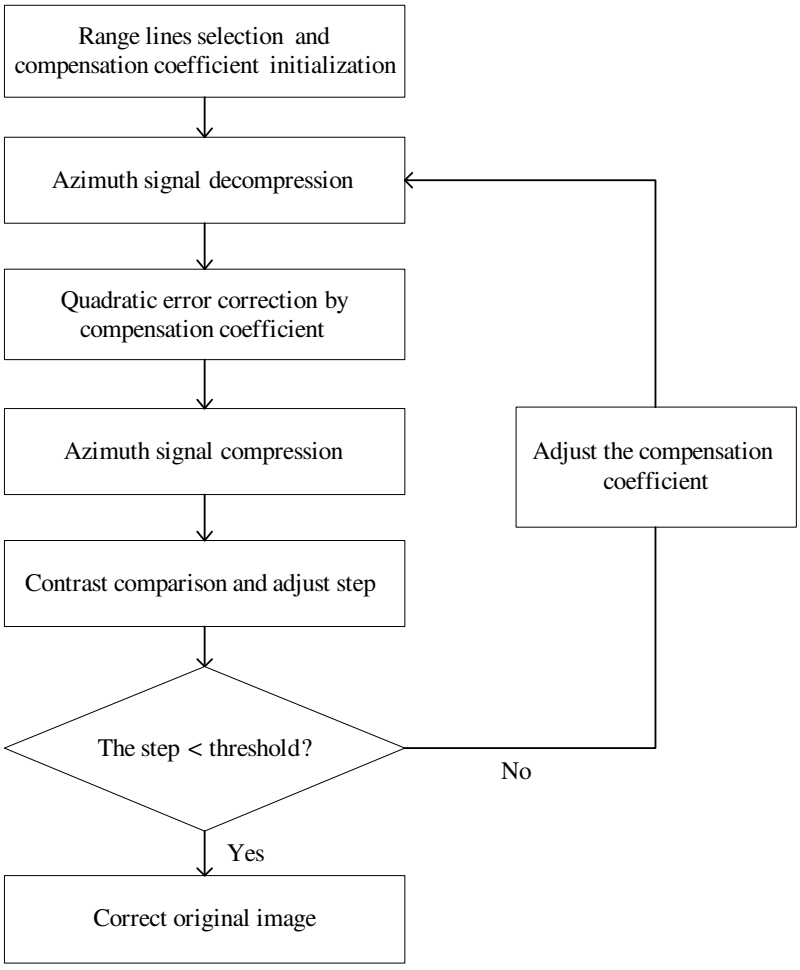

Figure 5. Flowchart of COA algorithm.

5. SIMULATIONS BASED ON PALSAR2 DATA

We test the effectiveness of COA using simulations based on ALOS PALSAR2 data, so that the image properties are representative of real scenes. The image is decompressed as GEO SAR Doppler history with integration time 520 s, and time-variant TEC error is induced to the azimuth signal.

Figure 6(a) shows an original image (an urban scene from Vancouver). Vertical direction is azimuth, and horizontal direction is range. Fig. 6(b) shows the image corrupted by time-variant TEC error with a quadratic coefficient -6.28×10^{-6} (at LT 18 on Mar. 6, 2016, from Lat.42° and Lon.−76°). Fig. 6(c) shows the image after COA compensation. We can see that due to the TEC error strong scatterers in the image are defocused, and after compensation they are refocused. The estimated quadratic coefficient is -6.15×10^{-6}, and the residual QPE is only 7.4°. Another original image (a mountain scene from Vancouver) is shown in Fig. 7(a). Same error as Fig. 6(b) is induced to the image. The images before and after compensation are shown in Figs. 7(b) and 7(c), respectively. It can be seen from the stripes in the image that after compensation the image is refocused. The estimated quadratic coefficient is -6.42×10^{-6}, and the residual QPE is only 8°.

Simulations with TEC quadratic coefficient 8.6×10^{-7} and 2.8×10^{-6} are implemented. 8.6×10^{-7} is the error bound (see Table 2), and 2.8×10^{-6} is maximum quadratic coefficient at Lat.43°, Lon.−100° when ascending node time is LT 18. The results of urban and mountain scenes are shown in Table 4. It can be seen that all the residual QPEs are far less than 45°, which indicates that after COA the image is refocused.

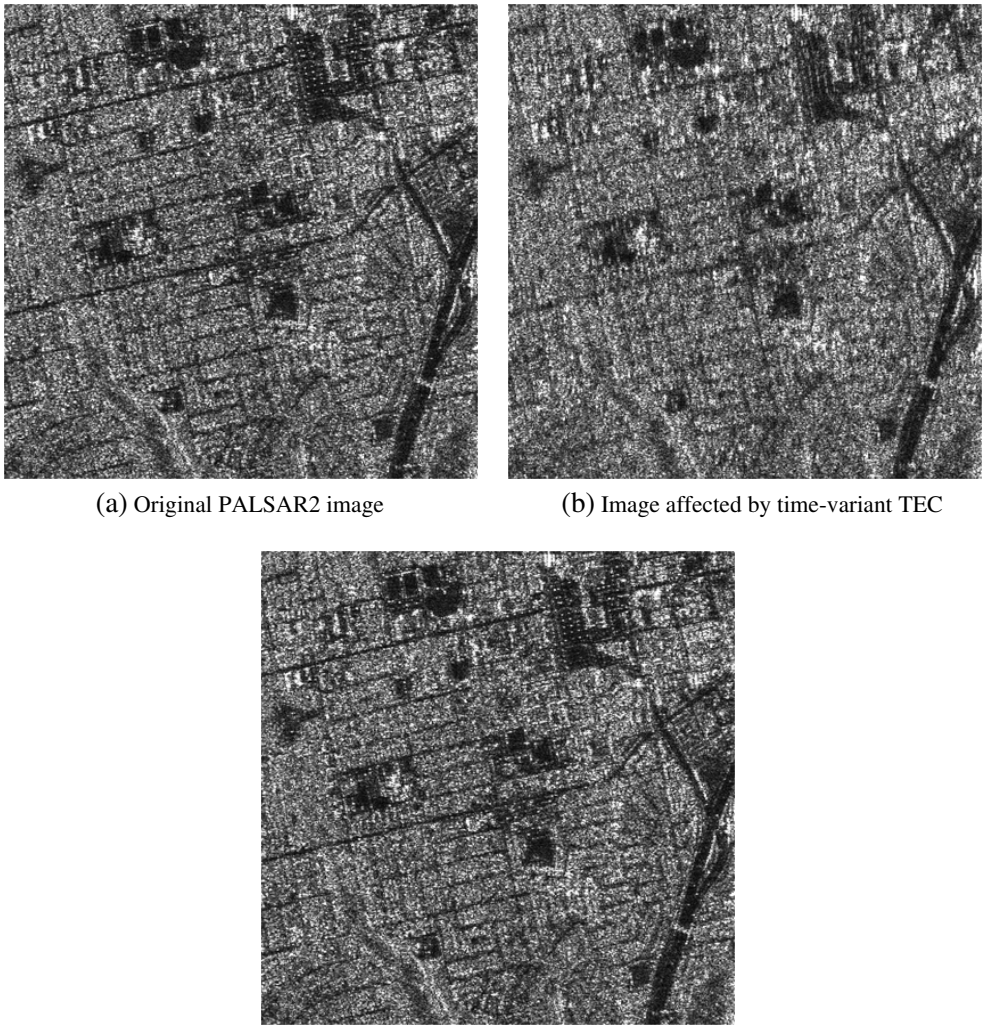

(a) Original PALSAR2 image (b) Image affected by time-variant TEC

(c) Image after COA compensation

Figure 6. Urban scene simulation result.

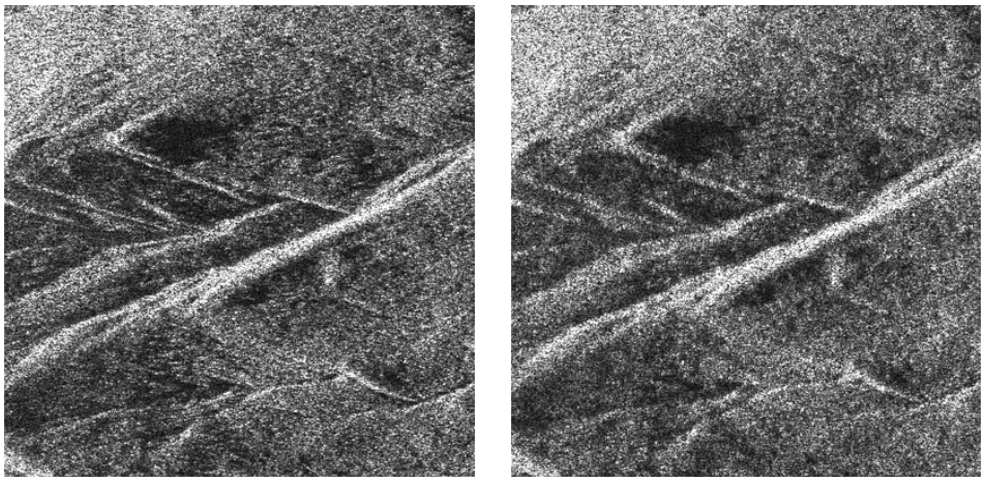

(a) Original PALSAR2 image (b) Image affected by time-variant TEC

(c) Image after COA compensation

Figure 7. Mountain scene simulation result.

Table 4. Simulation results.

	Urban scene		Mountain scene	
Induced coefficient (TECU/s^2)	8.6×10^{-7}	2.8×10^{-6}	8.6×10^{-7}	2.8×10^{-6}
Estimated coefficient (TECU/s^2)	9.86×10^{-7}	2.94×10^{-6}	1.00×10^{-6}	2.95×10^{-6}
Residual QPE	7.1°	7.7°	8.1°	8.4°

6. CONCLUSION

GEO SAR focusing suffers from ionospheric time-variant TEC due to its long integration time. A phase error is induced to the azimuth signal, which will make the SAR image defocused. Using USTEC data in whole 2016 TEC variation with time is analyzed. The quadratic phase error caused by time-variant TEC will exceed the focusing threshold, but cubic error can be ignored. Therefore, quadratic error is main effect on GEO SAR focusing, and COA algorithm can be used for compensation. The key steps of COA are presented. Its effectiveness is demonstrated using simulations based on scenes derived from PALSAR2 data.

ACKNOWLEDGMENT

This work was supported in part by the National Natural Science Foundation of China (NSFC) under Grant 61801442 and in part by the Fundamental Research Funds for the Central Universities, China under Grant 2652017111.

REFERENCES

1. Tomiyasu, K., "Synthetic aperture radar in geosynchronous orbit," *Proc. IEEE Antennas Propag. Symp.*, 42–45, 1978.
2. Bruno, D., S. E. Hobbs, and G. Ottavianelli, "Geosynchronous synthetic aperture radar: Concept design, properties and possible applications," *Acta Astronaut*, Vol. 59, 149–156, 2006.
3. Zhao, B., X. Qi, H. Song, W. Gao, X. Han, and R. P. Chen, "The accurate fourth-order doppler parameter calculation and analysis for geosynchronous SAR," *Progress In Electromagnetics Research*, Vol. 140, 91–104, 2013.

4. Zeng, T., W. Yang, Z. Ding, D. Liu, and T. Long, "A refined two-dimensional nonlinear chirp scaling algorithm for geosynchronous earth orbit SAR," *Progress In Electromagnetics Research*, Vol. 143, 19–46, 2013.
5. Yu, Z., P. Lin, P. Xiao, et al., "Correcting spatial variance of RCM for GEO SAR imaging based on time-frequency scaling," *Sensors*, Vol. 16, No. 7, 1091, 2016.
6. Guarnieri, A. M., S. Tebaldini, F. Rocca, et al., "Geosynchronous SAR for earth monitoring by interferometry and imaging," *IEEE International Geoscience and Remote Sensing Symposium (IGARSS)*, 210–213, 2012.
7. Hu, C., Y. Tian, X. P. Yang, et al., "Background ionosphere effects on geosynchronous SAR focusing: Theoretical analysis and verification based on the BeiDou navigation satellite system (BDS)," *IEEE Journal of Selected Topics in Applied Earth Observation and Remote Sensing*, Vol. 9, No. 3, 1143–1162, 2016.
8. Tian, Y., C. Hu, X. C. Dong, et al., "Theoretical analysis and verification of time variation of background ionosphere on geosynchronous SAR imaging," *IEEE Geoscience and Remote Sensing Letters*, Vol. 12, No. 4, 721–725, 2015.
9. Chen, J. and Z. Li, "Simultaneous measurement of time-variant TEC for compensating ionospheric effect on geosynchronous SAR using HF-radar," *IEEE 13th International Conference on Signal Processing (ICSP)*, 87–90, 2016.
10. Zhang, Q. B., Z. Yu, and P. Xiao, "Impacts of ionospheric temporal variability on L-band GEO SAR Imaging," *IEEE International Geoscience and Remote Sensing Symposium (IGARSS)*, 1194–1197, 2016.
11. Belcher, D. P. and N. C. Rogers, "Theory and simulation of ionospheric effects on synthetic aperture radar," *IET Radar Sonar Navig.*, Vol. 3, No. 5, 541–551, 2009.
12. Jehle, M., O. Frey, D. Small, et al., "Measurement of ionospheric TEC in spaceborne SAR data," *IEEE Transactions on Geoscience and Remote Sensing*, Vol. 48, No. 6, 2460–2468, 2010.
13. Carrara, W. G., R. S. Goodman, and R. M. Majewski, *Spotlight Synthetic Aperture Radar: Signal Processing Algorithms*, Artech House, Boston and London, 1995.